ICC
Iranian Chemical Communication
Original Research Article
Payame Noor University http://icc.journals.pnu.ac.ir

The theoretical study of adsorption HCN gas on the surface of pristine, Ge, P and GeP-doped (4, 4) armchair BNNTs

Mahdi Rezaei-Sameti*, Fateme Ataeifar

Department of Applied Chemistry, Faculty of Science, Malayer University, Malayer, 65174, Iran

Received: 4 August 2016, Accepted: 15 May 2017, Published: 15 May 2017

Abstract

In this research, the effects of HCN adsorption on the surface of the pristine, Ge, P, and GeP doped boron nitride nanotube (BNNTs) are investigated by using density function theory at the B3LYP/6–31G(d, p) level of theory. At the first step, we consider different configurations for adsorbing HCN molecule on the surface of BNNTs. The optimized models are used to calculate the structural, electrical, NQR parameters and quantum descriptors such as global hardness, global softness, electrophilicity, gap energy, Fermi level energy, electronic chemical potential, and electronegativity of BNNTs/HCN complex. Inspection of results demonstrates that with doping Ge impurity the sensitivity of BNNTs for adsorbing HCN molecule will significantly increase considering original values. The adsorption of HCN molecule on the surface of Ge-doped is more stable and favourable than other models. With HCN gas absorption and doping of Ge and GeP the NQR, quantum molecular descriptors and molecular orbital energies of the nanotube/HCN complex alter significantly from pristine nanotube. Comparing results reveal that the electrophilicity index of E model is more than those other models.

Keywords: BNNTs; HCN adsorption; DFT; NQR; DOS.

Introduction

Hydrogen cyanide (HCN) is a toxic liquid or colorless gas which boils at 26 ^{o}C. It is produced from the smoke of various tobacco and nitrogen containing organic materials [1]. Hydrogen cyanide is a poison compound and it can also be taken up through the skin [2]. It is highly lethal to man and animals, since it inhibits the consumption of oxygen by the bodily tissue. Therefore, it is important to develop sensitive sensors to detect the presence of toxic HCN [3–5]. In the recent years, the theoretical research show that the defective CNTs , BNNTs, SiCNTs, BC2NNTs and graphene are suitable as sensors in detecting HCN[6–11]. The results obtained by Zhang et al. [7] and Wang et al. [8] showed that B-doped on CNTs and Si-doped BNNTs can be respectively used as good sensors to detect HCN. Peyghan et al. proposed that Al doped BC2N nanotube can improve the sensitivity of the tube to HCN [9]. Rastegar et al. showed that Si- and Al-doped graphene improves the strength of the interaction of HCN gas with graphene [11]. Boron nitride nanotubes (BNNTs) were theoretically predicted in 1994 [12–13] and experimentally realized in the following year [14]. BNNTs have a good piezoelectricity,

*Corresponding author: Mahdi Rezaei-Sameti
Tel: +98 (851) 2355389, Fax: +98 (851) 2355389
E-mail: mrsameti@gmail.com

elastic, optical properties, photoelectric and thermal conductivity, the structures of defective single-walled BNNTs, as well as the doping [15–19]. The functionalization of the BNNTs with some groups such as H , F , CCl_2 , and NH_3, (H_2NNO_2) have been investigated in previous theoretical works, finding that these functional groups modify the electronic properties of the tubes in different ways of single-walled BNNTs and adsorption onto them have been reviewed [20–23]. The adsorptions of small molecules (i.e., H_2, NO, N_2O, O_2, CO, CO_2, C_2H_4, C_2H_2, H_2O and NH_3) on to pristine and doped BNNTs were studied using density functional theory (DFT) [24–30].

In the previous research, we studied the AsGa, Ga, C doped on BPNTs and AlNNTs, AlPNTs and CO adsorption on BPNTs [31–36]. The aims of this research is to investigate the effects of Ge, P, GeP on the adsorption of HCN gas on the surface of boron nitride nanotubes (BNNTs) in order to reveal some clues for chemical sensor design. For these aims, at the first step we consider eight models for adsorption HCN on the surface of pristine, Ge, P, GeP doped of BNNTs: (A) Vertical adsorption of HCN molecule on the B site of pristine BNNTs via nitrogen head, (B) Vertical adsorption of HCN molecule on the N site of pristine BNNTs via nitrogen head, (C) Vertical adsorption of HCN molecule on the B site of Ge–doped BNNTs via nitrogen head, (D) Vertical adsorption of HCN molecule on the N site of Ge–doped BNNTs via nitrogen head, (E) Vertical adsorption of HCN molecule on the B site of P–doped BNNTs via nitrogen head, (F) Vertical adsorption of HCN molecule on the N site of P–doped BNNTs via nitrogen head, (G) Vertical adsorption of HCN molecule on the B site of GeP–doped BNNTs via nitrogen head and (H) Vertical adsorption of HCN molecule on the N site of GeP–doped BNNTs via nitrogen head (Figure 1). All structures of nanotube/HCN complex models (A–H) have been optimized, and then, the electronic structure properties, quantum parameters, adsorption energies, band gaps, HOMO and LUMO orbitals and NQR parameters for all models are calculated and results are analysed.

Computational methods

In the first step, all representative (A–H) models of (4, 4) armchair single-walled BNNTs are allowed to relax by all atomic geometrical parameters in the optimization at the DFT level of B3LYP exchange functional and 6-31G (d, p) standard basis set using the GAMESS suite of programs [37]. Adsorption energy (E_{ads}) of HCN molecule on the pristine and Ge, P, GeP-doped BNNTs is calculated as follows:

$$E_{ads} = E_{BNNTs-CO} - (E_{BNNTs} + E_{HCN}) + BSSE \quad (1)$$

where $E_{BNNTs-HCN}$ obtained from the scan of the potential energy of the BNNTs–HCN, E_{BNNTs} is the energy of the optimized BNNTs structure, and E_{HCN} is the energy of an optimized HCN and BSSE is Base set superposition error. The quantum molecular descriptors electronic, chemical potential (μ), global hardness (η), electrophilicity index (ω), energy gap, global softness (S), Fermi level (E_{FL}), and electronegativity (χ) of the nanotubes are calculated as follows:

$$\mu = -(I + A)/2 \quad (2)$$

$$\eta = (I - A)/2 \quad (3)$$

$$\chi = -\mu \quad (4)$$

$$\omega = \mu^2/2\eta \quad (5)$$

$$S = 1/2\eta \quad (6)$$

$$E_{FL} = \frac{E_{HOMO} + E_{LUMO}}{2} \quad (7)$$

$$\Delta N = \frac{-\mu}{\eta} \quad (8)$$

$$\Delta E_{gap} = E_{LUMO} - E_{HOMO} \quad (9)$$

$$C_Q\ (MHZ) = e^2 Q q_{zz} h^{-1} \quad (10)$$

where I ($-E_{HOMO}$) is the ionization potential and A ($-E_{LUMO}$) the electron affinity of the molecule. The electrophilicity index is a measure of the electrophilicity power of a molecule [31–36, 38–44]. The NQR parameters (C_Q, η_Q) are determined as above the level of theory. The NQR parameters refer to the interaction energy of the nuclear electric quadrupole moment and the EFG tensors at the site of quadrupole nucleus. Eqs. (10, 11) are used to convert the EFG tensors to the measurable parameters C_Q and η_Q [45]. The standard Q values of ^{11}B and ^{15}N atoms are 40.59 and 20.11 *mb* respectively [46].

$$C_Q\ (MHZ) = e^2 Q q_{zz} h^{-1}$$

$$\eta_Q = \left|(q_{xx} - q_{yy})/q_{zz}\right| \quad (11)$$

$$(q_{zz} > q_{yy} > q_{xx}) \qquad 0 < \eta_Q < 1$$

Q is nuclear electric quadrupole moment and q_{zz} is the Z component of the EFG tensor in the principal axes system.

Results and discussion

Geometrical parameters HCN adsorption on BNNTs

From optimized structures of considered eight models (A–H) (See Fig.1), the structural parameters such as: the bond lengths of (B–N) and bond angles (B–N–B) of the pristine, Ge, P and GeP–doped of (4, 4) armchair BNNTs are detected and results are tabulated in Table 1.

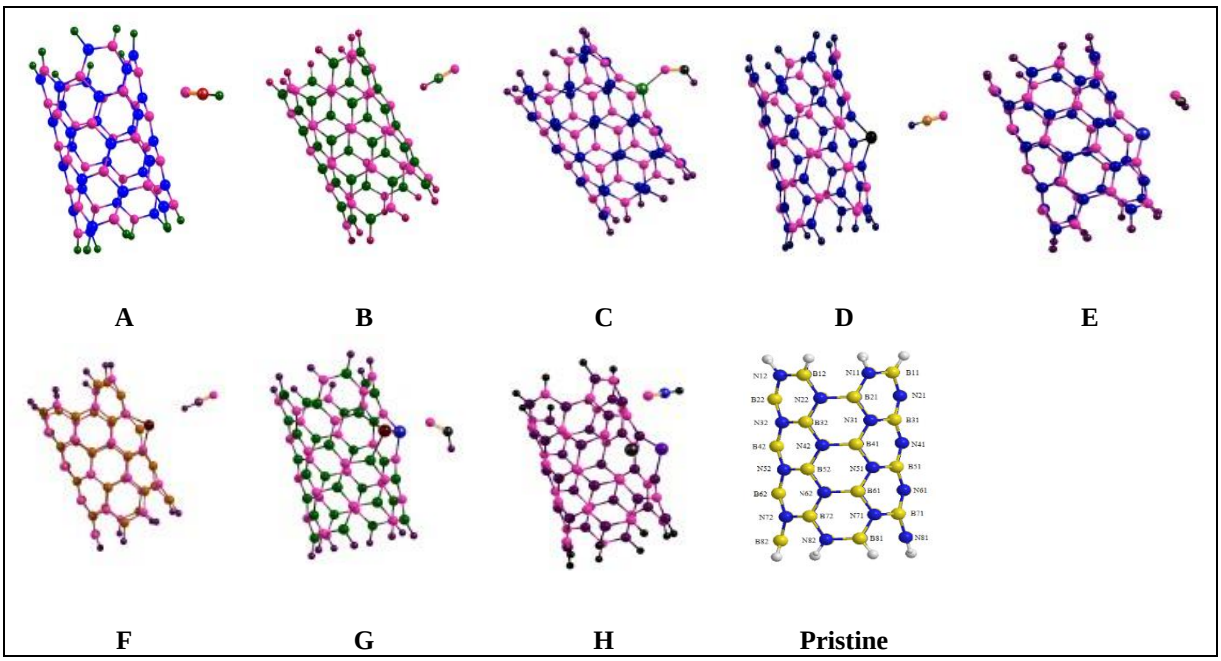

Figure 1. 2D views of pristine and Ge, P, GeP doped of (4, 4) armchair model of BNNTs for (A-H) models for adsorption HCN and pristine BNNTs

The average B–N bond length of armchair forms of BNNTs is 1.45Å, which is in agreement with other studies [16–19]. With doping Ge, P atoms on the site of the B41 and N42 of (4, 4) armchair form of BNNTs (See Fig .1), the bond lengths between N31–Ge, B32–P and Ge–P are 1.84, 1.90 and 2.28 Å respectively. By adsorbing HCN molecule on the surface of pristine, Ge, P and GeP–doped BNNTs ((A–H) models) the bond length changes slightly from the original values. Comparing the results reveals that doping of Ge and P atoms ~~have~~ has a significant effect on the charge transfer from B and N atoms and yielding asymmetric electronic charge density distribution along Ge–N and B–P bonds. Moreover the adsorption of HCN molecule on the surface of BNNTs slightly changed the charge transfer between B and N atoms and therefore the bond length is slightly altered. The bond angles of neighbor of P and Ge atoms at all models decrease from the original values. The radius of Ge and P atoms is more than B and N atoms and therefore doping of P and Ge atoms cause that the neighbor atoms of doping is agglomerated and the bond angles is decreased.

Table 1. Structural parameters of adsorption HCN molecule on the surface pristine and Ge, P, GeP doped of BNNTs models (A-H fig. 1)

Bond length(Å)	**Mode A**	**Model B**	**Model C**	**Model D**	**Model E**	**Model F**	**Model G**	**Model H**
B_{41}/Ge-N_{42}/P	1.45	1.45	1.83	1.87	1.95	1.95	2.28	2.35
B_{41}/Ge-N_{31}	1.45	1.45	1.81	1.84	1.47	1.45	1.83	1.86
B_{41}/Ge-N_{51}	1.45	1.45	1.81	1.83	1.46	1.46	1.83	1.85
N_{42}/P-B_{32}	1.45	1.45	1.44	1.44	1.90	1.90	1.93	1.92
N_{42}/P-B_{52}	1.45	1.45	1.44	1.44	1.90	1.90	1.92	1.92
N_{52}-B_{52}	1.45	1.45	1.44	1.45	1.45	1.45	1.44	1.45
Bond angel(°)								
B_{41}/Ge-P/N_{42}-B_{52}	115	115	114	114	89.2	89.2	90.4	90.5
B_{32}-P/N_{42}-B_{41}/Ge	114	114	113	113	89.2	89.2	90.1	90.5
B_{32}-P/N_{42}-B_{52}	119	119	121	122	97.8	97.8	96.8	96.8
N_{31}-B_{41}/Ge-N_{51}	119	119	106	103	121	121	104	100
N_{31}-N_{41}/Ge—P/N_{42}	119	119	104	101	119	119	109	105
N_{51}-B_{41}/Ge-P/N_{42}	120	120	105	102	118	118	110	107

The adsorption energy for HCN/BNNTs complex is calculated by Eq.1 and results are in given Table 2 and Figure 2. The adsorption energy of HCN/BNNTs complex is in the range of –10.92 to –1.63 eV. The adsorption energies of (A–H) models are negative and all adsorption process is exothermic and is favorable in thermodynamic approach. Among the (A–H) adsorption models the C model in thermodynamically approach is the most stable with negative E (ads) of –10.92 eV and lower distance of HCN to nanotube 1.84 Å. E_{ads} of the C and G models are –1.63 eV with distance 2.77 Å and are more unstable than other those models.

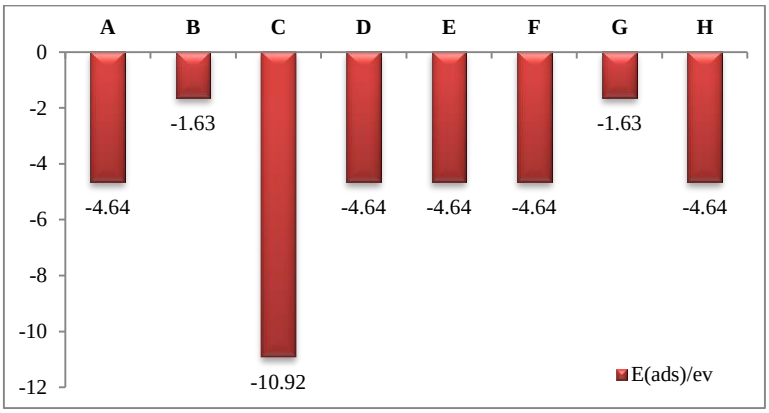

Figure 2. The graph of adsorption energy of pristine and Ge, P, GeP doped (A-H) models BNNTs (see Figure 1)

The results reveal that vertical adsorption of HCN molecule on the N site of pristine BNNTs via nitrogen head and GeP–doped BNNTs via nitrogen head are more unfavorable than other models and doping Ge decrease adsorption of HCN on the surface of BNNTs. The adsorption of HCN molecule on the surface of BNNTs is physisorption process due to weak van der Waals interaction between the nanotube and the HCN molecule. The BSSE values of all systems are in range 0.002–0.004 eV.

Table 2. Quantum parameters of HCN adsorption HCN on the surface of (4,4) armchair BNNTs (models A – H, Figure 1)

	A	**B**	**C**	**D**	**E**	**F**	**G**	**H**
E(HOMO)/ev	-6.33	-5.04	-6.05	-4.77	-6.64	-5.61	-6.63	-5.14
E(LUMO)/ev	-0. 27	-0.65	-0.36	-0.72	-0.26	-0.019	-0.99	-0.38
E(ads)/ev	-4.64	-10.92	-1.63	-4.64	-4.64	-4.64	-1.63	-4.64
I/ev	6.33	5.04	6.05	4.77	6.64	5.61	6.63	5.14
A/ev	0.027	0.65	0.36	0.72	0.26	0.019	0.99	0.38
μ/ev	-3.18	-2.84	-3.21	-2.74	-3.45	-2.81	-3.81	-2.76
χ/ev	3.18	2.84	3.21	2.74	3.45	2.81	3.81	2.76
η/ev	3.15	2.20	2.84	2.02	3.19	2.80	2.81	2.37
S/(ev)-1	0.16	0.23	0.18	0.25	0.15	0.17	0.18	0.21
ω/ev	1.60	1.84	1.81	1.87	3.73	1.42	2.57	1.60
ΔE(gap)/ev	6.30	4.40	5.09	4.05	6.38	5.60	5.63	4.75
BSSE	0.001	0.002	0.002	0.003	0.002	0.004	0.003	0.002
ΔN	1.01	1.29	1.13	1.36	1.08	1.01	1.44	1.16

Quantum molecular descriptors

To study the effects of HCN adsorption on the surface of pristine ,Ge, P and GeP doped on distribution of electron density of BNNTs, the highest occupied molecular orbital (HOMO) and the lowest unoccupied molecular orbital (LUMO) are calculated using B3LYP/6–31G (d, p) and results are shown in Figure 3. Notation 1 and 2 is used for HOMO and LUMO orbitals at all models (A–H). Figure 3 shows that at A and B models the density of HOMO orbitals are distributed on the center of nanotube near the HCN adsorption and LUMO orbitals are

located on the head nanotube, due to donor electron effect of a lone pair electron of nitrogen atom of HCN. By doping Ge, P and GeP atoms the HOMO orbitals at C-1, D-1, E-1, F-1, G-1 and H-1models are located on the center of nanotube near HCN adsorption and doping area; Moreover the LUMO orbitals at C-2, D-2, E-2, H-2 are localized on the surface of HCN molecule. The comparison results reveal that by doping Ge, P, and GeP atoms and adsorbing HCN the density of electrons are pervaded on the surface of nanotube. From the HOMO/LUMO orbitals results, the densities of states (DOS plot) for all models are determined in energy range –10 to 5 eV by using GaussSum program [47] and are shown in Figure 4. The comparisons made on DOS plots of all models reveal that the number of DOS peak at the HOMO region is five peaks and at the LUMO region are seven peaks.

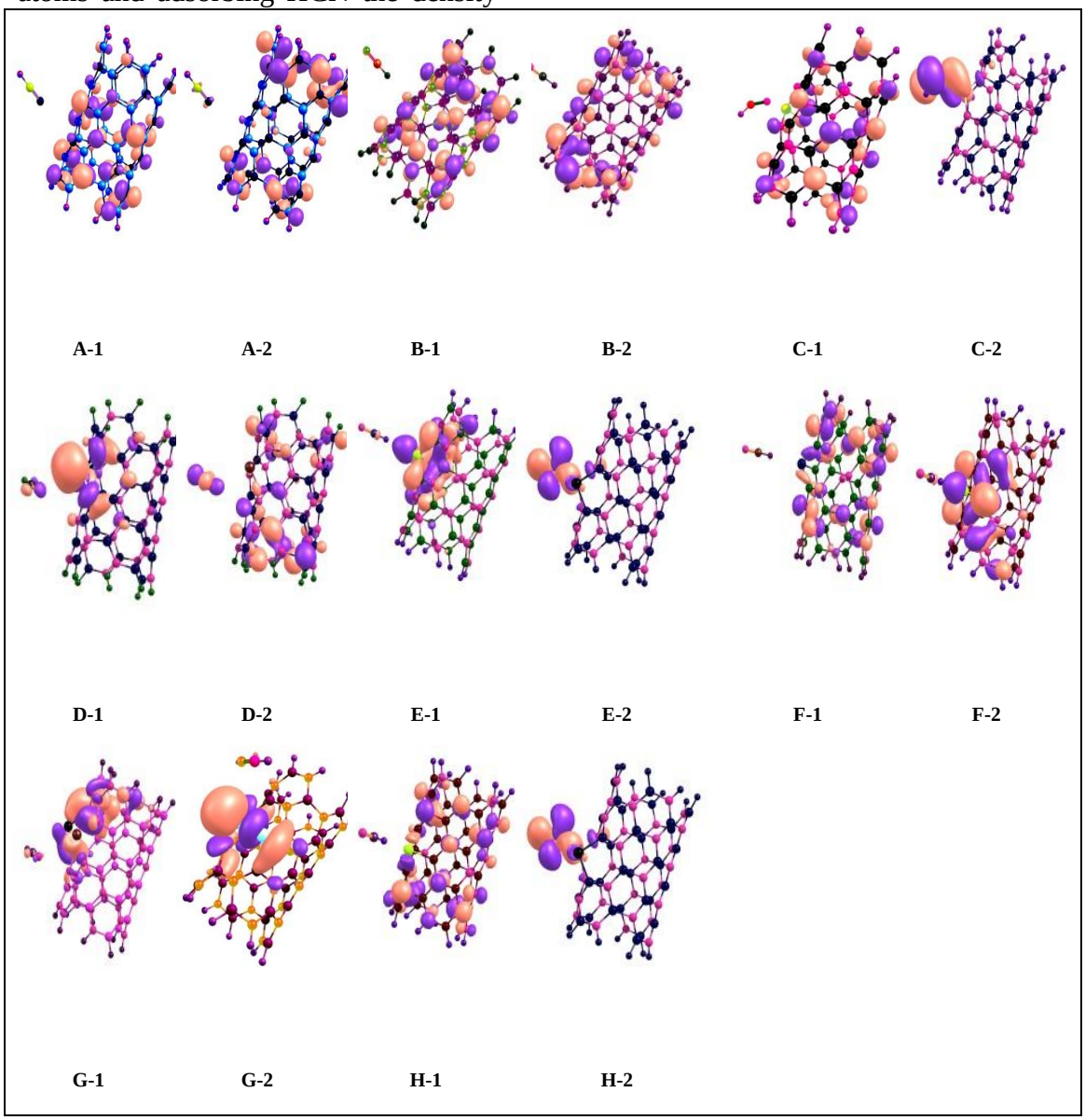

Figure 3. Plots of HOMO and LUMO structures of HCN adsorption on the pristine and Ge, P, GeP doped (A-H)models of BNNTs , notation 1 and 2 indicate HOMO and LUMO orbital respectively (see Figure 1)

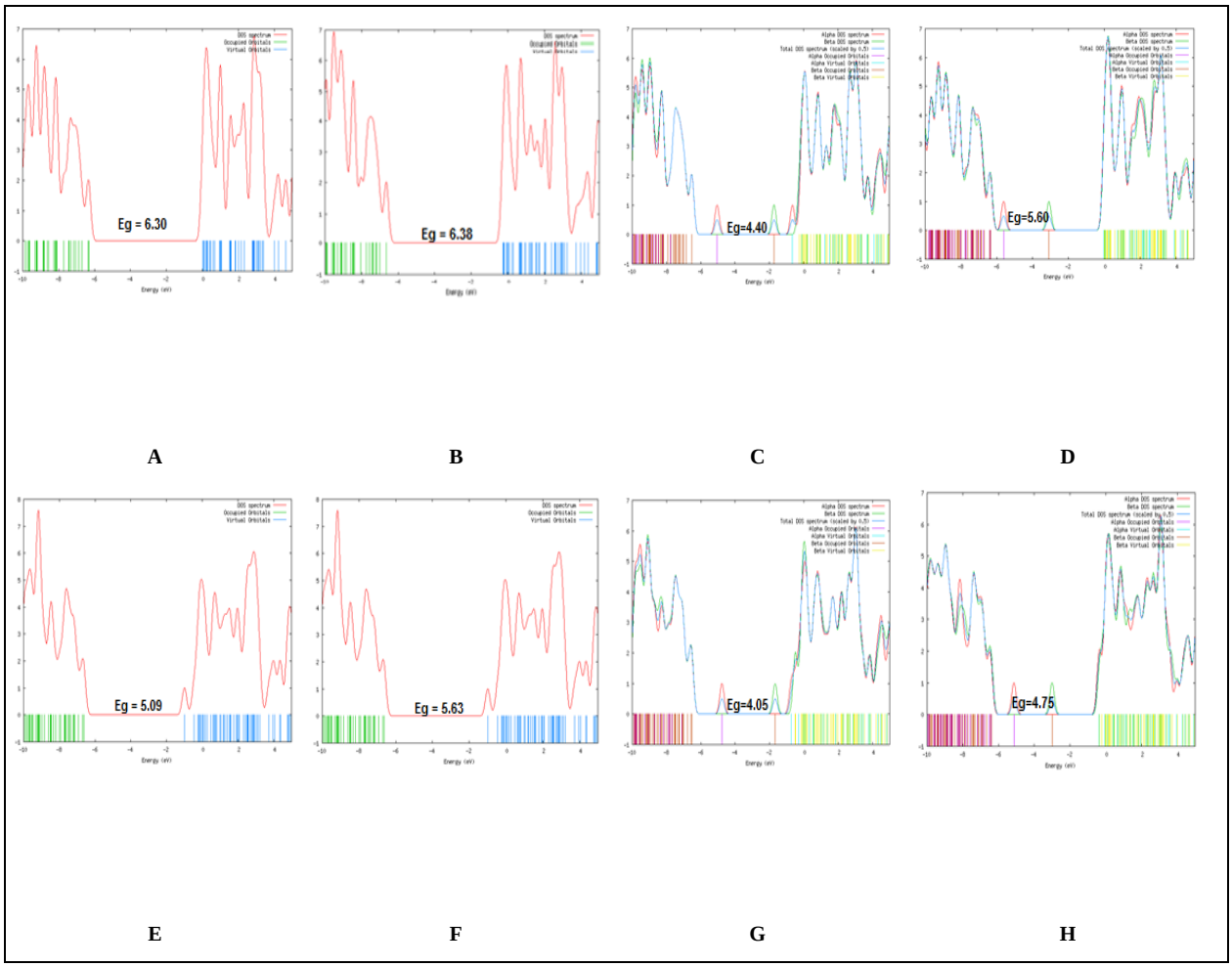

Figure 4. DOS Plots of HCN adsorption on the pristine and Ge, P, GeP doped (A-H) models BNNTs (see Figure 1)

By doping Ge , P and GeP atoms the altitude of all pecks decrease significantly from pristine models, and so the photoelectric properties of all doped nanotube decrease from original form. By doping Ge and GeP atoms on the C, D, G and H models two peaks is engendered between HOMO and LUMO area and caused that the gap energy decrease significantly from other models, it can be concluded that a semiconductor properties of these models increase. The gap energy between HOMO and LUMO orbitals is calculated by Eqs. 9 and results are given in Table 1 and shown in Figure 6. The calculated results of Figure 6 show that the gap energy is dependent to configuration of HCN adsorption on the surface of pristine, Ge, P and GeP doped BNNTs. The comparison of results show that gap energy of A and E models are 6.30 and 6.38 eV respectively and are more than other models and gap energy of D model is 4.05 eV and is lower than other models. The gap energy for adsorption of HCN on the N site of BNNTs via nitrogen head is lower than B site. This lowering of gap energy may be able to increase the reactivity of complexes and show charge transfer to take place between the HCN molecule and nanotube. These results are useful to devise sensors for detecting HCN molecule in the environmental pollutions. The quantum

molecular descriptors electronic, chemical potential electron (μ), global hardness(η), global softness (S), electrophilicity index (ω), energy gap (E_{gap}), Fermi level (E_{FL}), and electronegativity (χ) of the nanotubes are calculated and results are given in Table 2 and Figures (5, 6).

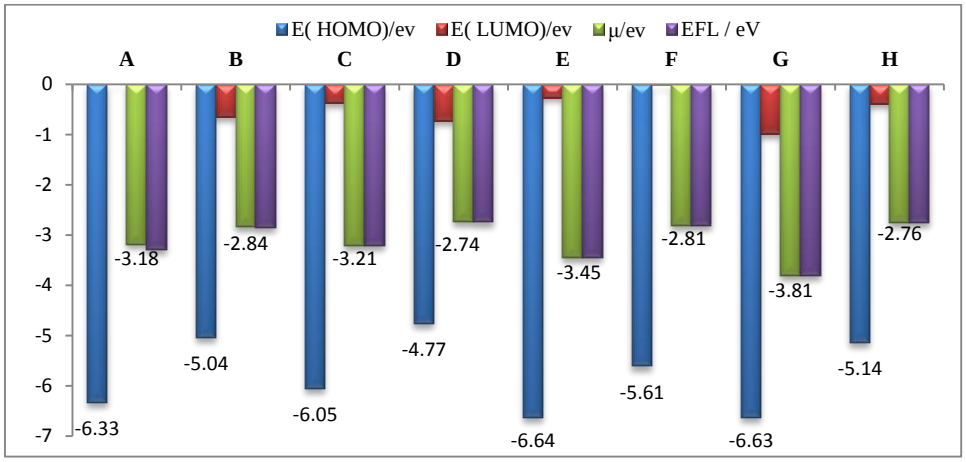

Figure 5. The graph of energy level of HOMO, LUMO, Fermi level, Chemical potential of pristine and Ge, P, GeP doped (A-H) models BNNTs (see Figure 1)

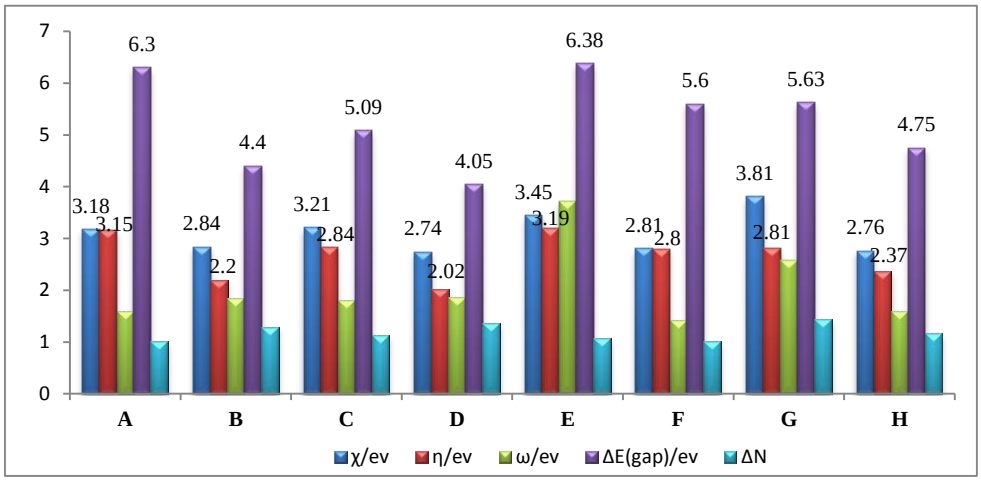

Figure 6. The graph of energy level global hardness(η), electrophilicity index (ω), energy gap (E_{gap}), charge transfer (ΔN) and electronegativity (χ) of of pristine and Ge, P, GeP doped (A-H) models BNNTs (see Figure 1)

The chemical potential electron (μ) is change in free energy when electrons are added or removed from the system. In the case of electrons, the chemical potential is usually expressed in energy per particle rather than energy per mole, and the energy per particle is conventionally given in units of electron volt (eV) in Table 2. Chemical potential plays an especially important role in semiconductor physics. The negative values of chemical potential show that the charges transfer between two particles are spontaneously. The chemical potential of electrons in solids is closely related to the concepts of work function, Fermi level, electronegativity, and ionization potential. In fact, the chemical potential of an atom is sometimes said to be the negative of the atom's electronegativity. Likewise, the

process of chemical potential equalization is sometimes referred to as the process of electronegativity equalization. In this work the chemical potential electron (μ) for all models is negative in range of –2.74 to −3.81 eV and reveals that the charge transfer occurs between nanotube and HCN molecule. The charge transfer between HCN molecule and BNNTs at G model is more than other models. The amount of charge transfer (ΔN) between the HCN molecule and BNNTs is calculated using the equation (8) and given in Table 2 and Figure 6. ΔN values of (A–H) models are positive in range of 1.01 to 1.36 eV and indicate that HCN molecule act as an electron acceptor. The global hardness (η) of (A–H) models is calculated by Eq. 3 and results are given in Figure 6. The global hardness of (A–H) models in range 2.02 to 3.19 eV. The global harness of D model is lower than the other models; on the other hand it depends to configuration of HCN adsorption and doping of atoms. By doping Ge and GeP doped the global hardness decreases from pristine model and so the stability of nanotube decrease. The electrophilicity index (ω) of (A–H) models is calculated by Eq. 5 and results are shown in Figure 6. The electrophilicity index (ω) of E model is more than other models and H model is lower than other those models. The electrophilicity index (ω) determines maximum flow of electron from donor to acceptor species and supplies data connected to structural stability, reactivity and toxicity of chemisorbed on the surface of nanotube, a fairly large charge transfer occurs between two related species, thus their electronic transport properties could be significantly changed upon physisorption of HCN.

The nuclear quadrupole resonance parameters of ^{11}B and ^{15}N

Nuclear quadrupole resonance spectroscopy (NQR) is a chemical analysis technique. NQR transitions of nuclei can be detected in the absence of a magnetic field, and for this reason NQR spectroscopy is referred to as "zero Field NMR." The NQR resonance is mediated by the interaction of the electric field gradient (EFG) with the quadrupole moment of the nuclear charge distribution. It is this product which is termed the nuclear quadrupole coupling constant for a given isotope in a material and can be found in tables of known NQR transitions. The NQR parameters of ^{11}B and ^{15}N nuclei at different sites of (A–H) models are calculated by Eqs. (10 and 11) and results are tabulated in Table 3 and Figures 7 and 8.

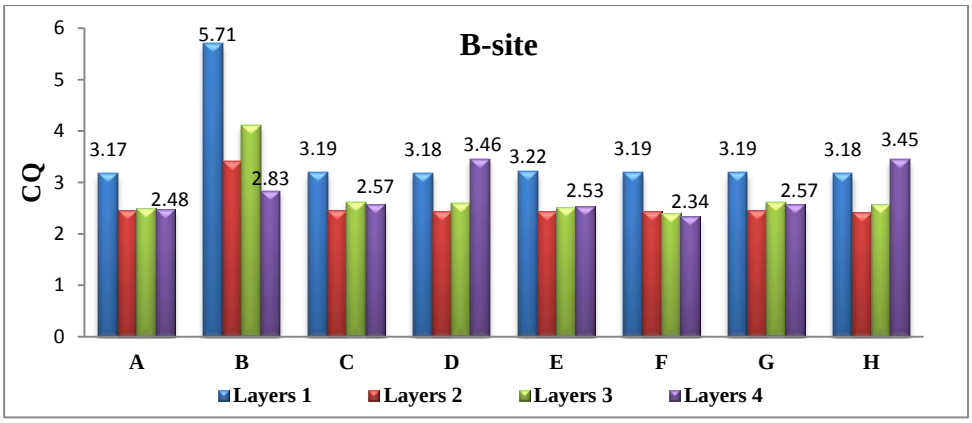

Figure 7. The CQ parameters for B nuclei of pristine and Ge, P, GeP doped (A-H) models BNNTs (see Figure 1)

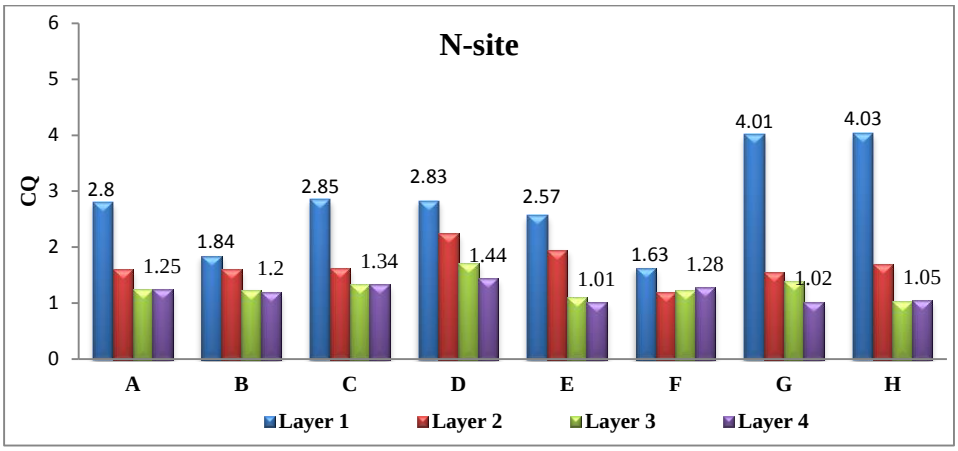

Figure 8. The CQ parameters for N nuclei of pristine and Ge, P, GeP doped (A-H) models BNNTs (see Figure 1)

The nuclear quadrupole coupling (*CQ*) of 32 B and 32 N atoms in all (A–H) models are separated into four layers based on the similarity of the calculated electric field gradient (EFG) tensors in each layer; therefore, the electrostatic environment of the BNNTs is equivalent along each layer. As shown in Figures (7 and 8) the C*Q* values of the first layer for B and N nuclei for all models are more than other those layers. The results reveal that the orientation of the EFG tensor eigenvalues along the z–axis of the first layer is stronger than the other layers along the length of the nanotube. Moreover the fourth layer has the low C_Q among of other layers in alone nanotube.

Table 3. NQR parameters of HCN adsorption HCN on the surface of pristine and Ge, P, Ge-P doped (4,4) armchair BNNTs and adsorption models A-H (see Figure 1)

	Prinstin		**Ge Doped**		**P Doped**		**Ge-p Doped**	
	CQ	**ηQ**	**CQ**	**ηQ**	**CQ**	**ηQ**	**CQ**	**ηQ**
Layer1	3.24	0.19	3.19	0.17	3.14	0.17	3.17	0.17
Layer2	2.43	0.02	2.45	0.03	2.46	0.03	2.41	0.03
Layer3	2.48	0.05	2.45	0.05	2.65	0.04	2.58	0.05
Layer4	3.51	0.06	3.48	0.05	3.51	0.05	3.45	0.04
NQR parametrs N-Atom								
Layer1	3.03	0. 95	2.85	0.86	2.86	0.87	2.38	0.85
Layer2	1.68	0.56	1.65	0.51	1.62	0.64	1.70	0.43
Layer3	1.49	0.52	2.16	0.57	1.33	0.14	2.12	0.31
Layer4	1.55	0.38	1.79	0.40	1.34	0.42	1.41	0.34
NQR parameters B -Atom								
	A		**B**		**C**		**D**	
Layer1	3.17	0.16	5.71	0.54	3.19	0.18	3.18	0.17
Layer2	2.46	0.03	3.42	0.55	2.46	0.03	2.45	0.03

Layer3	2.49	0.04	4.12	0.92	2.62	0.03	2.59	0.05
Layer4	2.48	0.04	2.83	0.40	2.57	0.09	3.46	0.05
NQR parameters N-Atom								
Layer1	1.60	0. 09	1.24	0.04	2.85	0.88	2.83	0.86
Layer2	1.24	0.57	1.61	0.17	1.62	0.64	1.71	0.43
Layer3	1.25	0.53	1.84	0.34	1.33	0.14	2.24	0.27
Layer4	1.25	0.37	1.20	0.05	1.34	0.42	1.44	0.27
NQR parameters B -Atom								
	E		**F**		**G**		**H**	
Layer1	3.22	0.17	3.19	0.17	3.19	0.18	3.18	0.16
Layer2	2.44	0.02	2.44	0.03	2.46	0.03	2.42	0.03
Layer3	2.52	0.06	2.40	0.05	2.62	0.03	2.57	0.04
Layer4	2.53	0.06	2.34	0.05	2.57	0.09	3.45	0.04
NQR parameters N-Atom								
Layer1	2.57	0.63	1.63	0.39	4.00	0.93	4.03	0.97
Layer2	1.00	0.31	1.20	0.41	1.55	0.41	1.70	0.67
Layer3	1.10	0.40	1.23	0.25	1.40	0.25	1.03	0.21
Layer4	1.95	0.06	1.28	0.92	1.02	0.92	1.05	0.75

The significant difference between NQR parameters at the first layer and the fourth layer is due to the change of the geometrical parameters. The comparison results of Figure (7) reveal that the C*Q* parameters of first layer for B nuclei at the B model is 5.71 ppm and is more than other models due to donor electron effects of HCN adsorption on the N site of BNNTs. On the other hand the C*Q* parameters of first layer for N nuclei at G and H models are 4.01 and 4.03 ppm respectively and are more than other those models (see Fig 8). The donor electron effect of GeP doped and HCN adsorption cause that the density of electron around N site of first layer is more than other layers, this result is in agreement of HOMO orbital density at first layers of the models B, G and H.

Conclusion

In this research we have presented studies of interaction between the HCN molecule and pristine, Ge, P and GeP doped BNNTs. The structural, electrical, HOMO-LUMO, quantum parameters and NQR parameters for eight models (A–H) are investigated by using DFT theory. The calculated results indicate that the interaction between HCN molecule and BNNTs is physisorption and the adsorption energy of HCN/BNNTs complex is in the range of –10.92 to –1.63 eV. The adsorption energy of the C model is more negative than other those models with lower distance of HCN to nanotube 1.84 Å. With doping Ge atom the sensitivity of BNNTs to adsorption of HCN increase significantly from pristine model. Thereby Ge doped BNNTs is a good candidate to adsorb and make sensor for HCN molecule. The positive values of ΔN show that HCN molecule act as an electron acceptor. By doping Ge and GeP atoms the global hardness of system decreases significantly from pristine models and so the reactivity of nanotube increases the HCN adsorption. The NQR

parameters indicate that the C*Q* parameters of first layer the G and H models are 4.01 and 4.03 ppm respectively and are more than other those models.

Acknowledgments

The authors thank the Centre of computational Nano of Malayer University for supporting this research.

References

[1] Hydrogen Cyanide - Compound Summary. Pub Chem Compound. USA: National Center for Biotechnology Information. 16 September, *http://pubchem.ncbi.nlm.nih.gov/compound /768*, **2004**.

[2] D. Dwork; R.J. van Pelt, *Auschwitz, 1270 to the present. Norton*, **1996**, 443.

[3] Hydrogen Cyanide. *Organization for the Prohibition of Chemical Weapons, Retrieved*, **2009**, 14.

[4] Hydrogen cyanide (CHEBI:18407). *Chemical Entities of Biological Interest. UK: European Bioinformatics Institute, 18 October, https://www.ebi.ac.uk/chebi/searchId.do/ chebiId=18407*, **2009**.

[5] P. Patnaik, Handbook of Inorganic Chemicals. *McGraw-Hill, ISBN 0-07-049439-8*, **2002**.

[6] M. Zhao, F. Yang, Y. Xue, D. Xiao, Y. Guo, *J. Mol. Model*, **2014**, *20*, 2214–2218.

[7] Y.M. Zhang, D.J. Zhang, C.B. Liu, *J. Phys. Chem B.*, **2006**, *110*, 4671–4674.

[8] R.X. Wang, D.J. Zhang, Y.J. Liu, C.B. Liu, *Nanotechnology*, **2009**, *20*, 505704–10.

[9] A. A. Peyghan, N. L. Hadipour , Z. Bagheri, *J. Phys. Chem C*, **2013**, *117*, 2427–2432.

[10] R.Q. Wu, M. Yang, Y.H. Lu, Y.P. Feng, Z.Q. Huang, Q.Y.Wu, *J. Phys. Chem C*, **2008**,*112*, 15985–15988.

[11] S.F. Rastegar, A.A. Peyghan, N. L. Hadipour, *Appl. Surf. Sci*, **2013**, *265*, 412–417.

[12] A. Rubio, J.L. Corkill, M.L. Cohen, *Phys. Rev. B*, **1994**, *49*, 5081–5084.

[13] X. Blase, A. Rubio, S.G. Louie, M.L. Cohen, *Europhys. Lett*, **1994**, *28*, 335– 340.

[14] N.G. Chopra, R.J. Luyken, K. Cherrey , V.H. Crespi , M.L. Cohen , S. G. Louie and A. Zettl, *Science*, **1995**, *269*, 966–967 .

[15] Y. Li, Z. Zhou, D. Golberg, Y. Bando, P.R. Schleyer, Z. Chen, *J. Phys. Chem C*, **2008**, *112*, 1365–1370.

[16] G. Kim, J. Park, S. Hong, *Chem. Phys. Lett*, **2012**, *522*, 79–82.

[17] C.C. Tang , Y. Bando , C.H. Liu, S.S. Fan, J. Zhang, X.X. Ding, D. Golberg, *J. Phys. Chem B*, **2006**, *110*, 10354–7 .

[18] S. Tontapha, V. Ruangpornvisuti, B. Wanno, *J. Mol. Model*, **2013**, *19*, 239–245.

[19] S.M. Nakhmanson, A. Calzolari, V. Meunier, J. Bernholc, M.B. Nardelli, *Phys. Rev. B*, **2003**, *67*, 235406 –10.

[20] X. Wu, W. An, X.C. Zeng, *J. Am. Chem. Soc*, **2006**, *128*, 12001–6.

[21] X.J. Wu, J.L. Yang, J.G. Hou, Q.S. Zhu, *Phys. Rev. B*, **2004**, *69*, 153411–14.

[22] H.J. Xiang, J.L. Yang, J.G. Hou, Q. S. Zhu, *Appl. Phys. Lett*, **2005**, *87*, 243113–243115.

[23] Y. Li, Z. Zhou, J. Zhao, *Nanotechnology*, **2008**, *19*, 015202–7.

[24] A. Ahmadi, J. Beheshtian, L.N. Hadipour, *Struct. Chem*, **2011**, *22*, 183–188.

[25] J. Zhao, Y. Ding, *J. Phys. Chem. C*, **2008**, *112*, 20206–11.

[26] M.T. Baei, *Monatsh. Chem*, **2012**, *143*, 989–995.

[27] Y. Xie, Y.P. Huo, J.M. Zhang, *Appl. Surf. Sci*, **2012**, *258*, 6391–6397.

[28] X.M. Li, W.Q. Tian, X.P. Huang, C.C. Sun, L. Jiang, *J. Mol. Struct (THEOCHEM)*, **2009**, *901*, 103–109.
[29] M.T. Baei, A.R. Soltani, A.V. Moradi, E.T. Lemeski, *Compt. Theo. Chem*, **2011**, *970*, 30–35.
[30] J. Beheshtian, Z. Bagheri, M. Kamfiroozi, A. Ahmadi, *Microelectron. J*, **2011**, *42*, 1400–1403.
[31] M. Rezaei Sameti, *Physica E*, **2010**, *43*, 588–592.
[32] M. Rezaei-Sameti, *Physica B*, **2012**, *407*, 22–26.
[33] M. Rezaei-Sameti, *Physica E*, **2012**, *44*, 1770–1775.
[34] M. Rezaei-Sameti, *Quantum Matter*, **2013**, *2*, 1–5.
[35] M. Rezaei-Sameti, S. Yaghobi, *Phys. Chem. Res*., **2013**, *1*, 90–98.
[36] M. Rezaei-Sameti, A. Kazemi, *Turk J Phys*, **2015**, *39*, 128–136.
[37] M.W. Schmidt, K.K. Baldridge, J.A. Boatz, S.T. Elbert, M.S. Gordon, J.H. Jensen, S. Koseki, N. Matsunaga, K.A. Nguyen, S.J. Su, T.L. Windus, M. Dupuis, J.A. Montgomery, General atomic and molecular electronic structure system. *J. Comput. Chem*, **1993**, *14*, 1347–1363.
[38] R. Ditchfield, W.J. Hehre, J.A. Pople, *J. Chem. Phys*, **1972**, *54*, 724–728.
[39] M.T. Baei, M. Moghimi, P. Torabi, A. Varasteh Moradi, *Comp. Theo. Chem*, **2011**, *972*, 14–19.
[40] P.K. Chattaraj, U. Sarkar, D.R. Roy, *Chem. Rev*, **2006**, *106*, 2065–2091.
[41] K.K. Hazarika, N.C. Baruah, R.C. Deka, *Stru. Chem*, **2009**, *20*, 1079–1085.
[42] R.G. Parr, L. Szentpaly, S. Liu, *J. Am. Chem. Soc*, **1999**, *121*, 1922–1924.
[43] R.G. Pearson, *J. Chem. Sci*, **2005**, *111*, 369–377.
[44] B.C. Gerstein, C.R. Dybowski, Transient Techniques in NMR of Solids; Academic Press: New York, **1985**.
[45] P. Pyykkö, *Mol. Phys*, **2001**, *99*, 1617–1629.
[46] T. Koopmans, *Physica*, **1933**, *1*, 104.
[47] C. Tabtimsai , S. Keawwangchai, N. Nunthaboot, V. Ruangpornvisuti, B. Wanno, *J. Mol. Model*, **2012**, *18*, 3941–3949.